



FULL LENGTH ARTICLE

Cathepsin K contributed to disturbed flow-induced atherosclerosis is dependent on integrin-actin cytoskeleton—NF- κ B pathway



Fei Fang ^a, Tang Feng ^a, Jianwei Li ^b, Huaiyi Zhang ^a, Qin Wang ^b, Yidan Chen ^c, Guixue Wang ^c, Yang Shen ^{a,**}, Xiaoheng Liu ^{a,*}

^a Institute of Biomedical Engineering, West China School of Basic Medical Sciences & Forensic Medicine, Sichuan University, Chengdu, Sichuan 610041, China

^b Department of Endocrinology and Metabolism, West China Hospital, Sichuan University, Chengdu, Sichuan 610041, China

^c Key Laboratory for Biorheological Science and Technology of Ministry of Education, State and Local Joint Engineering Laboratory for Vascular Implants, College of Bioengineering, Chongqing University, Chongqing 400030, China

Received 10 January 2022; received in revised form 7 March 2022; accepted 22 March 2022
Available online 25 April 2022

KEYWORDS

Atherosclerosis;
Cathepsin K;
Disturbed flow;
Integrin;
NF- κ B

Abstract Atherosclerosis is a chronic inflammatory disease, occurring preferentially in bifurcation, branching, and bending of blood vessels exposed to disturbed flow. Disturbed flow in atheroprone areas activates elevated proteases, degrading elastin lamellae and collagenous matrix, resulting in endothelial dysfunction and vascular remodeling. As a mediator for extracellular matrix protein degradation, cathepsin K (CTSK) was directly regulated by hemodynamics and contributed to atherosclerosis. The mechanism of CTSK responding to disturbed flow and contributing to disturbed flow-induced atherosclerosis is unclear. In this study, the partial carotid ligation model of mice and *in vitro* disturbed shear stress model were constructed to explore the contribution and potential mechanism of CTSK in atherosclerosis. Our results indicated that CTSK elevated in the disturbed flow area *in vivo* and *in vitro* along with endothelial inflammation and atherogenesis. Additionally, the expression of integrin α v β 3 was upregulated in these atheroprone areas. We found that inhibition of the integrin α v β 3-cytoskeleton pathway could significantly block the activation of NF- κ B and the expression of CTSK. Collectively, our findings unraveled that disturbed flow induces increased CTSK expression, and contributes to endothelial inflammation and vascular remodeling, leading to

* Corresponding author.

** Corresponding author.

E-mail addresses: shenyang@scu.edu.cn (Y. Shen), liuxiaohg@scu.edu.cn (X. Liu).

Peer review under responsibility of Chongqing Medical University.

atherogenesis eventually. This study is helpful to provide new enlightenment for the therapy of atherosclerosis.

© 2022 The Authors. Publishing services by Elsevier B.V. on behalf of KeAi Communications Co., Ltd. This is an open access article under the CC BY-NC-ND license (<http://creativecommons.org/licenses/by-nc-nd/4.0/>).

Introduction

Atherosclerosis is a complex vascular inflammatory disease characterized by lipid accumulation, plaque formation, and artery stenosis, which remains the leading cause of vascular diseases worldwide.¹ Due to being constantly exposed to blood flow, the vascular heterogeneity and homeostasis were regulated by different flow velocities and patterns. The endothelial cell layer senses laminar flow in most arterial regions and exerts atheroprotective functions. However, exposure to disturbed blood flow leads to endothelial dysfunction and inflammation in arteries bifurcation, curvatures, and branch areas.^{2,3} It is known that endothelial inflammation-induced vascular remodeling plays a vital role in atherogenesis. The adaptive and compensatory remodeling is understood as compensation of luminal modulation to delay plaque development.

Atherosclerosis induced by disturbed flow promotes endothelial dysfunction, activates elevated levels of proteases, and modulates the arterial matrix's composition, resulting in vascular remodeling and the formation of atherosclerotic plaques eventually. Vascular remodeling is associated with elastin lamellae and collagenous matrix degradation and redistribution of extracellular matrix (ECM).⁴ The classical view is that matrix metalloproteinases (MMPs) belong to a family of proteases known as the metzincin superfamily and degrade all kinds of ECM proteins. Besides, cathepsin K (CTSK), one of the most potent proteases in lysosomal cysteine proteases belonging to the peptidase protein C1 family, is confirmed to be involved in the redistribution of ECM in the process of atherosclerosis.⁵ Recently, CTSK has been reported expressed in the endothelial cells, macrophages, and vascular smooth muscle cells of human atherosclerotic lesions.⁶ The high colocalization of CTSK and CTSK-generated C-telopeptides of type I collagen was found in the neointima and atherosclerotic shoulders, providing strong evidence that CTSK contributed to the vascular remodeling and the formation of atherosclerotic plaques.⁷ It has been found that CTSK was regulated by oxidized LDL (OxLDL),⁸ cytokines,^{9,10} and oscillating shear stress.¹¹ However, the molecular mechanism of how hemodynamics transmits and regulates CTSK expression is not well understood.

As an essential candidate of biomechanical sensors, integrins play a central role in transducing the mechanical stimuli into biochemical signals. Integrin clusters facilitate dynamic linkages between the cytoplasmic tails of the β subunit and the intracellular actin cytoskeleton assemble to focal adhesion plaques formation and cytoskeletal arrangement. In addition, the assembly of endothelial actin has been implicated in pathological inflammatory

responses. A previous study identified integrin $\alpha v \beta 3$ as a primary flow-induced NF- κ B activation and contributed to early atherogenic inflammation.¹² To investigate the molecular mechanisms of CTSK in regulating disturbed flow-induced atherogenesis. The partial carotid ligation mice model was constructed to explore the mechanism of disturbed flow-induced CTSK participating in endothelial inflammation and vascular remodeling. The expression levels of $\alpha v \beta 3$ integrin and CTSK in atheroprone areas and activation of NF- κ B were examined. Our results demonstrated that CTSK contributed to flow-dependent endothelial inflammation and vascular remodeling, which are expected to be inhibited by targeting integrin $\alpha v \beta 3$ -cytoskeleton. This study is helpful to provide new enlightenment for the therapy of atherosclerosis.

Materials and methods

Cell culture

The Human umbilical vein vessel endothelial cells (HUVECs, Jiangsu Blood Research Institute) were cultured in RPMI-1640 (GIBCO), including 10% fetal bovine serum (FBS, GIBCO), penicillin (100 U/mL), and streptomycin (100 mg/mL). All cell lines were cultured under an atmosphere of 5% CO₂ at 37 °C.

Animals

Male C57BL/6 mice and male apolipoprotein E knockout (*ApoE*^{-/-}) mice were obtained from the GemPharmatech Co., Ltd. Male mice (6–8 weeks) were used in this study. All mice have free access to water and food and are kept at a constant temperature of 25 °C. All animal work was performed with the approval of the Medical Ethics Committee of Sichuan University (K2021015). All ethical guidelines for experimental animals were followed. The atherosclerosis model was established with *ApoE*^{-/-} mice fed a high-fat diet (5 g per mouse per day, #D12108C, SYSEBIO Co).

Partial carotid ligation models

The partial carotid ligation model was performed as described previously.^{13,14} Briefly, the external carotid artery (ECA), occipital artery (OA), and internal carotid artery (ICA) of the left carotid artery (LCA) were ligated, leaving the superior thyroid artery (STA) intact. The ligation model could induce disturbed flow in LCA and aortic arch (AA) regions; on the contrary, the RCA and DA were laminar shear stress. All model mice were ligated for 21 days, the C57BL/6 were fed a normal diet, and the *ApoE*^{-/-} mice

were fed a high-fat diet. The test group was given *i.v.* With integrin inhibitor cilengitide (5 $\mu\text{g}/\text{kg}/\text{d}$) for 21 days, and the dimethyl sulfoxide vehicle (1:1 solution of dimethyl sulfoxide: PBS) as the control group.

Application of shear stress

HUVECs were seeded on gelatin-coated μ -slides for 8 hours. Laminar shear stress (LSS) was applied to HUVECs for 8 hours using a parallel plate flow chamber that generated 15 dyn/cm^2 of unidirectional flow.^{15,16} In addition, \pm 4.5 dyn/cm^2 of disturbed shear stress (DSS) was generated using a rocker model to simulate the pro-atherogenic flow.^{17,18} Briefly, the HUVECs were seeded in a 10-cm length of the Petri dish with 2.0-mm culture medium and placed in a rocker shaker with a tilt angle of 7° and a rocking frequency of 0.5 Hz.

In the experiment of inhabitation of integrin subunits, we used different integrin inhibitors (including 5 μM of integrin $\alpha\text{v}\beta 3$ inhibitor cilengitide for 12 hours, 5 μM of integrin $\alpha 4\beta 1/\alpha 4\beta 7$ inhibitor firtategrast for 1 hour, and 5 μM of integrin $\alpha 5\beta 1$ inhibitor ATN-161 for 12 hours, respectively) to pre-treat the HUVECs and then subject to the stimulation of LSS or DSS.

En face immunostaining

En face immunostaining was performed on the luminal side of the aortas and common carotid arteries as previously.¹⁹ Briefly, the aorta was isolated and dissected longitudinally. Dissected tissues were fixed in 4% paraformaldehyde for 4 hours and washed with 0.3% PBST (0.3% Triton X-100 in PBS) at room temperature three times (15 minutes/time). Subsequently, samples were blocked with 5% goat serum at 4 °C overnight. The aorta and carotid artery tissue sections were incubated with different antibodies for immunofluorescence analysis, including CTSK (1:300), CD31 (1:500), or p65 (1:300), respectively (Table S2). The nuclei were stained with DAPI dyes and observed under a confocal laser microscope (Zeiss, LSM710).

Western blotting

After homogenizing the isolated aorta and carotid artery or HUVECs under different flow conditions, the total protein was extracted with radioimmunoprecipitation assay (RIAP). The BCA protein assay determined the protein concentrations. Approximately 30 μg of protein was loaded on a 10% sodium dodecyl sulfate-polyacrylamide gel electrophoretically separated and electrophoretically transferred onto polyvinylidene fluoride (PVDF) membranes. After blocking Tris-buffered saline with 5% nonfat dry milk (phosphorylation antibody blocking with 5% bovine serum albumin), PVDF membranes were incubated overnight at 4 °C with primary antibodies, including CTSK (1:300), integrin αv (1:200), integrin $\beta 3$ (1:200), p65 (1:300), phosphorylation p65 (p-p65, 1:300) at 536, and GAPDH (glyceraldehyde 3-phosphate dehydrogenase, 1:1000) (Table S2). Then, HRP-conjugated secondary antibody was added and incubated at room for

1 hour. PVDF membranes were examined using the molecular image chemiDoc XRS + system (Bio-Rad Inc., USA).

RNA isolation and qRT-PCR

Total RNAs from shear stress treated HUVECs or RCA, LCA, DA, and AA in ligation mice were extracted by TRIzol reagent (Invitrogen, USA). To quantify CTSK expression levels, equal amounts of cDNA were synthesized using the Takara PrimeScript™ RT Master Mix (#RR036A, Takara, Japan). Quantitative real-time polymerase chain reaction (qRT-PCR) was done in triplicates in 20 μL of the brilliant SYBR green PCR master mixture (#4913914, Roche, Switzerland) and five pmol of both forward and reverse primers. GAPDH was amplified as an internal control. Sequences for the qRT-PCR primers are listed in Table S1.

Immunofluorescence staining

Immunofluorescence staining was performed for tissue sections or cells as recently reported.²⁰ Briefly, tissue sections or cells were fixed with 4% paraformaldehyde for 30 minutes. After blocking in 1% goat serum in PBS, samples were immune-stained with the antibodies as indicated, including CD31 (1:500), CTSK (1:300), integrin αv (1:200), and integrin $\beta 3$ (1:200), Col1-A (1:200), p65 (1:200) et al (Table S2). The nuclei were stained with DAPI dyes and observed under a confocal laser microscope.

Oil red O (ORO) staining

ApoE^{-/-} mice were euthanized after administration, and the aorta was isolated. Aorta was resected and perfused with 10% neutral buffered formalin for 2 hours. Carefully removing the periadventitial tissue and the atherosclerotic plaques of the aorta were detected by *en face* ORO staining. Quantitative analysis of atherosclerotic plaque areas was determined by software Image-Pro Plus 6.0 (National Institutes of Health, Bethesda, USA).

H&E staining

The aorta paraffin sections were deparaffinized, rehydrated, and stained with hematoxylin for 3 minutes. After washing with triple distilled water, the samples were stained with eosin for 1 minute. Next, the samples are dehydrated through graded alcohol. At last, the slides are mounted with neutral gum.

Van Gieson (VG) staining

The aorta paraffin sections were deparaffinized, rehydrated, and stained with weigert's hematoxylin for 20 minutes. After washing with water for 10 minutes, the samples were stained with Van Gieson's solution for 1 minute. Subsequently, we performed rapid dehydration with 95% alcohol and absolute alcohol, and mounted the slides with neutral gum.

Statistical analysis

All data are expressed as the mean \pm standard error (SE) in this study. IBM SPSS Statistics 26 (IBM, USA) was used for the statistical analysis. One-way ANOVA and Student's *t*-test were utilized for statistical analysis.

Results

Disturbed flow-induced vascular remodeling in *ApoE*^{-/-} mice

Firstly, we established the disturbed flow model using the classical partial carotid ligation model of *ApoE*^{-/-} mice (Fig. 1A). In this *in vivo* flow model, LCA and AA regions are exposed to disturbed flow, while the RCA and DA regions are exposed to a steady laminar flow. After 21 days of high-fat feeding after surgery, oil red O (ORO) staining results demonstrated that in the ligated LCA, the lipid deposition was significantly higher than that in sham groups (Fig. 1B, indicated by yellow arrows). H&E staining confirmed that the LCA lumen was obstructed by arterial wall thickening after 21-day ligation (Fig. 1C). In addition, the diameter of blood vessels in the ligation groups also increased significantly (Fig. 1D). Furthermore, the VG staining results showed that the thickness of the medial layer increased, and more broken elastic fibers were observed in the aortic medial layer in the ligated LCA compared to the sham group (Fig. 1E–G, as blue arrows indicated). These results demonstrated that the disturbed flow cloud induces fast atherosclerosis associated with excessive expansive vascular remodeling.

Disturbed flow-induced vascular inflammation is accompanied by vascular remodeling

To exclude the influence of serum cholesterol levels and lipid deposition on vascular inflammation and remodeling, we used normolipidemic mice's partial carotid ligation model to perform disturbed flow *in vivo*. We tested the hypothesis that NF- κ B is responsible for flow-induced cell inflammation. Therefore, we detected the translocation of p65, which plays a crucial role in the NF- κ B family, in ECs under different flow regions. As shown in Figure 2A, the p65 protein was mainly located in the cytoplasm of the laminar flow areas (RCA and DA) *in vivo*. However, the p65 protein was translocated into the nucleus in the LCA and AA regions (indicated by yellow arrows), demonstrating the activation of NF- κ B. Subsequently, we detected the mRNA levels of pro-inflammation cytokines in LCA, RCA regions from C57BL/6 mice 21 days after ligation. The qRT-PCR results showed that the inflammation-related mRNA (IL-1 β , IL-6, TNF- α , and p65) in the LCA region was significantly increased compared with the RCA region (Fig. 2B).

In addition, the H&E staining results demonstrated that disturbed flow leads to neointimal hyperplasia without lipid deposition in normolipidemic mice (Fig. 2C). As shown in Figure 2D, more elastin layer breaks were found in disturbed flow areas (LCA and AA region, as indicated by blue arrows). Taken together, these results revealed that

the vascular inflammation and remodeling induced by disturbed flow during the initiation and progression of atherogenesis are independent of serum cholesterol levels or lipid deposition in the arterial wall.

Upregulation of CTSK expression in the disturbed flow region

In the process of vascular remodeling, the migration of SMCs from the intima to the terminal is the leading cause of intimal thickening.²¹ The SMCs migration requires space for ECM redistribution. CTSK is one of the most potent proteases in the lysosomal cysteine proteases family and is involved in ECM degradation. It is reported that CTSK regulates inflammation response through TLR-9²² and TGF- β ²³ signaling pathways. Therefore, CTSK is probably involved in vascular remodeling and vascular inflammation induced by the disturbed flow. Firstly, we detected the distribution of CTSK and Col1-A in the ligated *ApoE*^{-/-} mice. As shown in Figure S1, we observed the co-localization of CTSK and Col1-A in the ligated group, indicating that CTSK may remodel the extracellular matrix by degrading type I collagen. *En face* immunofluorescence staining results showed that the expression of CTSK in ECs of disturbed flow areas (LCA, AA) was significantly higher than that of laminar flow areas (RCA, DA) of C57BL/6 mice 21 days after ligation (Fig. 3A). Furthermore, the protein and mRNA level of CTSK in LCA and AA regions was markedly increased than that of RCA and DA regions, respectively (Fig. 3B, C).

Disturbed flow increases integrin α v β 3 expression

Next, we investigated the molecular process underlying disturbed flow that induces CTSK in the pro-atherosclerosis area. Integrin plays an essential role in the mechano-transduction of hemodynamic forces to biochemical signals. Among them, integrin α v β 3 is a direct sensor of uni-directional flow for keeping vascular homeostasis.²⁴ Based on the previous research, the integrin is proposed as the mechanical mediator in disturbed flow, promoting the expression of CTSK. Therefore, we use a partial carotid ligation model to create disturbed flow in LCA and curved AA. Meanwhile, the RCA and DA regions served as control groups for disturbed flow due to their exposure to laminar blood flow. The immunofluorescence images showed that integrin α v and β 3 (labeled by red fluorescence) levels in LCA and AA of C57BL/6 mice 21 days after ligation were significantly higher than those in the RCA and DA groups (Fig. 4A, B).

DSS induces cell inflammation and increases CTSK expression *in vitro*

Furthermore, a parallel plate flow chamber and rocker model *in vitro* were used to generate unidirectional laminar shear stress (LSS) or disturbed shear stress (DSS). HUVECS were exposed to laminar shear stress (15 dyn/cm²) or disturbed shear stress (\pm 4.5 dyn/cm²) for 8 hours, respectively. As shown in Figure 5A, the expression levels of phosphorylation p65 at ser536, determined by Western blot, was elevated by DSS, compared with LSS or static

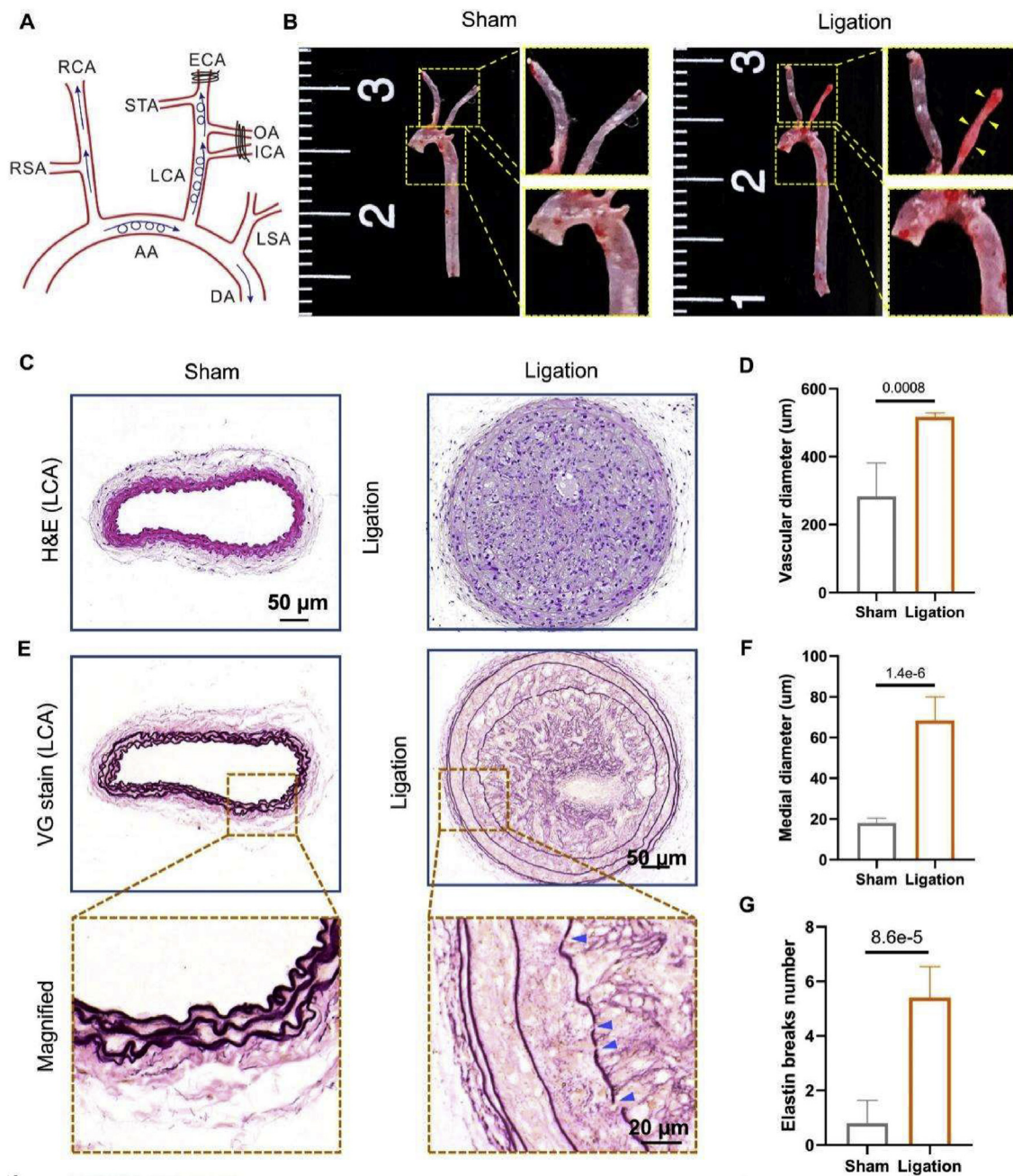


Figure 1 Disturbed flow induces atherosclerotic and vascular remodeling in the left carotid artery (LCA). (A) Schematic of partial carotid ligation surgery model. Right subclavian artery (RSA), right carotid artery (RCA), external carotid artery (ECA), superior thyroid artery (STA), occipital artery (OA), internal carotid artery (ICA), left carotid artery (LCA), left subclavian artery (LSA), aortic arch (AA), descending aorta (DA). (B) The arterial whole-mount ORO staining on the arteries harvested 21 days ligation from *ApoE*^{-/-} mice showed the lipid-rich plaques (red) in LCA, the lipid deposition as indicated by yellow arrows. (C) H&E staining of LCA sections from *ApoE*^{-/-} mice 21 days after ligation. (D) The vascular mean diameter of LCA tissue sections was measured by Image J software (*n* = 3). (E) VG staining of LCA sections from *ApoE*^{-/-} mice 21 days after ligation, the sites of elastic breaks as indicated by blue arrows. (F) Medial diameter and elastin break number (G) of VG-stained LCA tissue sections were measured by Image J software (*n* = 3).

control. *In vitro* study confirmed that the p65 protein translocated from cytoplasm to nucleus in HUVECs induced by DSS for 8 hours (Fig. 5B). The intensity curve showed the evident co-localization of p65 protein and the cell nucleus in the DSS condition compared with the LSS and

static control group (Fig. 5B). Because the phosphorylation of p65 protein invoked by DSS could promote NF-κB activation and lead to cell inflammation, we assessed the mRNA expression of pro-inflammatory mRNA in HUVECs under different flow conditions by qRT-PCR. The

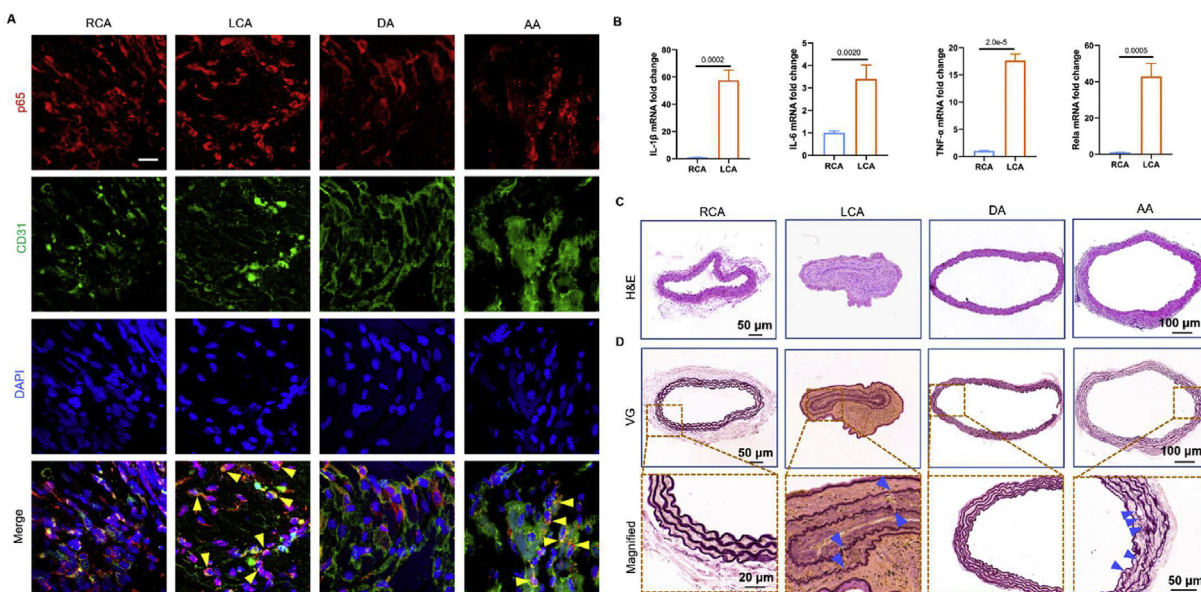


Figure 2 Disturbed flow induces vascular inflammation in normolipidemic mice. **(A)** *en face* staining of p65 (red) and CD31 (green) in RCA, LCA, DA, and AA regions from normolipidemic mice 21 days after ligation. DAPI stained the nucleus, and the images were captured by confocal microscopes (Scale bar: 20 μ m). **(B)** The mRNA expression levels (IL-1 β , IL-6, TNF- α , and p65) in RCA and LCA regions from mice 21 days after ligation were determined by qRT-PCR ($n = 3$). **(C)** H&E staining of RCA, LCA, DA, and AA sections from C57BL/6 mice 21 days after ligation, respectively. **(D)** VG staining of RCA, LCA, DA, and AA sections from C57BL/6 mice 21 days after ligation, respectively (elastin rupture sites were shown in blue arrow).

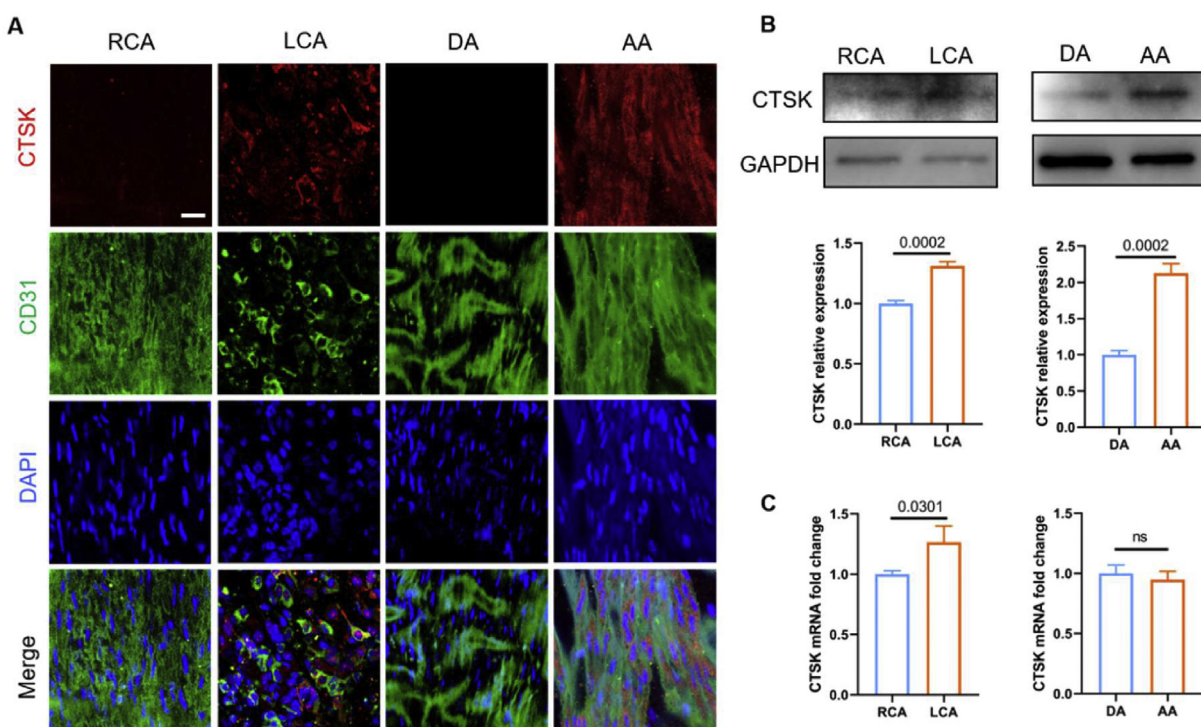


Figure 3 Disturbed flow promotes the expression of CTSK *in vivo*. **(A)** *En face* immunofluorescence staining for CTSK (red) and CD31 (ECs marker, green) on the RCA, LCA, DA, and AA of C57BL/6 mice 21 days after ligation, respectively. Nuclei were stained with DAPI, and the image was captured by a confocal microscope (Scale bar: 20 μ m). **(B, C)** The protein and mRNA expression levels of CTSK in the RCA, LCA, DA, and AA of C57BL/6 mice 21 days after ligation, respectively ($n = 3$).

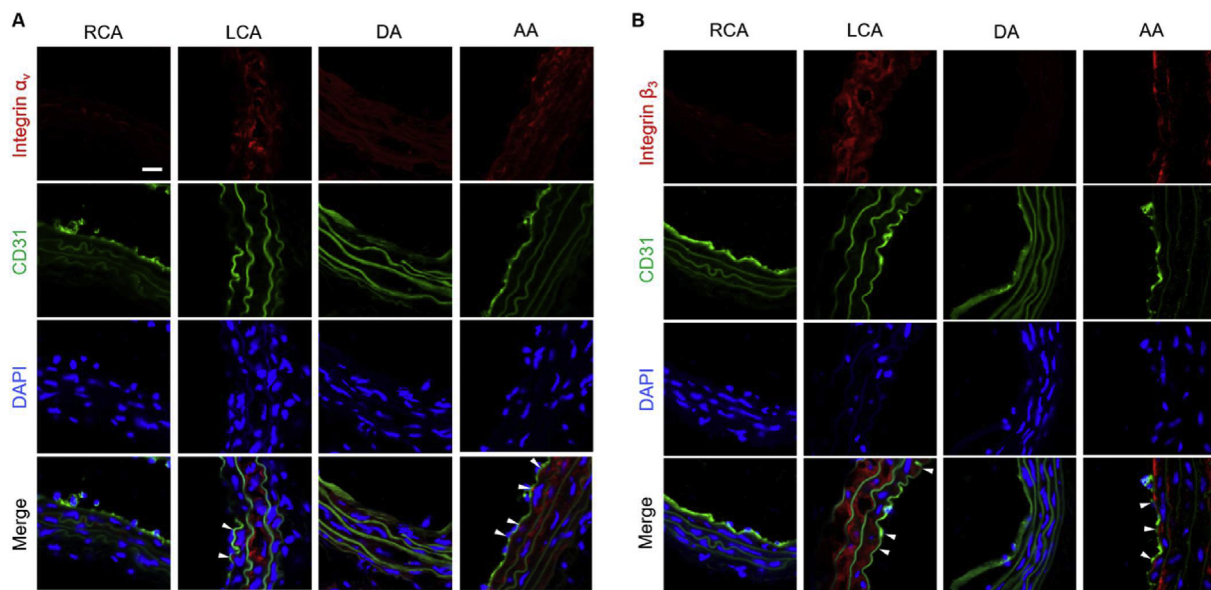


Figure 4 Disturbed flow upgraded the expression of integrins. Immunofluorescence staining for integrin αv (A) or $\beta 3$ (B) on the RCA, LCA, DA, and AA of C57BL/6 mice 21 days after ligation, respectively ($n = 3$). The endothelium was indicated by CD31 (ECs marker) with green fluorescence. Nuclei were stained with DAPI, and the image was captured by a confocal microscope (Scale bar: 20 μm). White arrows indicated the positive areas.

quantitative expression of mRNA (IL-1 β , IL-6, TNF- α , and IL-8) was markedly upregulated by DSS compared with LSS or static control (Fig. 5C).

Subsequently, we examined the expression of CTSK in HUVECs exposed to different flow conditions by Western blot. As shown in Figure 5D, it revealed that DSS significantly increased the level of CTSK in HUVECs compared with LSS and static control group, consistent with the results of *in vivo* model. The qRT-PCR results further confirmed that the mRNA expression of CTSK was markedly enhanced by DSS (Fig. 5E).

The type I collagen is the substrate of CTSK; the triple helix structure of type I collagen can be cleaved by CTSK. Accordingly, CTSK and type I collagen were labeled by red and green fluorescence. As shown in Figure 5F, prominent type I collagen filaments are observed in the static control and LSS group but significantly decreased with a high level of CTSK in the DSS group. These results indicated that the DSS could promote the expression of CTSK and degrade the matrix, leading to vascular remodeling eventually.

In addition, we found that the expression of integrin αv and $\beta 3$ in DSS groups was significantly increased than that in the LSS group or static control group (Fig. 5G). Taken together, our results demonstrated that DSS could induce endothelial inflammation and ECM redistribution, accompanied by high levels of CTSK and integrin $\alpha v\beta 3$.

Integrin-cytoskeleton mediates flow-induced NF- κB activation and vascular remodeling

We further elucidate how integrin mediates shear-induced atheroprone changes. As a downstream signal transduction element of integrins, the actin dynamics responded to different flow patterns, implicated to pathological inflammatory responses. Previous results indicated DSS

induced the translocation of p65 (Fig. 5B), which could be redistributed to the cytoplasm in the presence of cilengitide (a specific inhibitor of integrin $\alpha v\beta 3$), and ATN-161 (integrin $\alpha 5\beta 1$ inhibitor), suggesting that endothelial inflammation could be blunted entirely by inhibition of integrins. By using integrin inhibitor cilengitide or ATN-161 (integrin $\alpha 5\beta 1$ inhibitor), it could be found that there are no obvious differences of actin fiber (labeled by green fluorescence, Fig. 6A, B).

Interestingly, even if exposed to LSS, the p65 signal in HUVECs was activated with cilengitide pre-treatment for 12 hours. Similarly, inhibition of integrin $\alpha 4\beta 1/\alpha 4\beta 7$ with firsategrast showed the anti-inflammatory effects in HUVECs exposed to DSS, but pro-inflammatory effects in HUVECs in LSS treated group (Fig. S2).

The qRT-PCR results showed that the mRNA expression levels of the pro-inflammatory factors (IL-6, TNF- α , ICAM-1, p65, and IL-8) significantly decreased in the DSS groups than those in LSS groups with pre-blocking integrin (Fig. 6C). By contrast, exposure to LSS significantly enhanced the CTSK level by inhibiting integrin (Fig. 6D). The cytoskeleton polymerization inhibitors latrunculin B (LatB, 10 μM for 12 hours) was used to explore the integrin-induced cytoskeletal arrangement and inflammation under the different flow conditions. As shown in Figure S3A, cells displayed disordered actin stress with less and short pseudopodia at the leading edge of lamellipodia after inhibiting the cytoskeleton arrangement. Additionally, inhibition of cytoskeleton polymerization with the treatment of LatB strengthened flow-dependent endothelial inflammation. That is to say, LatB stimulation will further increase the retention of p65 protein in the cytoplasm in both static culture and LSS groups; in the DSS groups, LatB will promote the p65 protein to enter the nucleus (Fig. S3B).

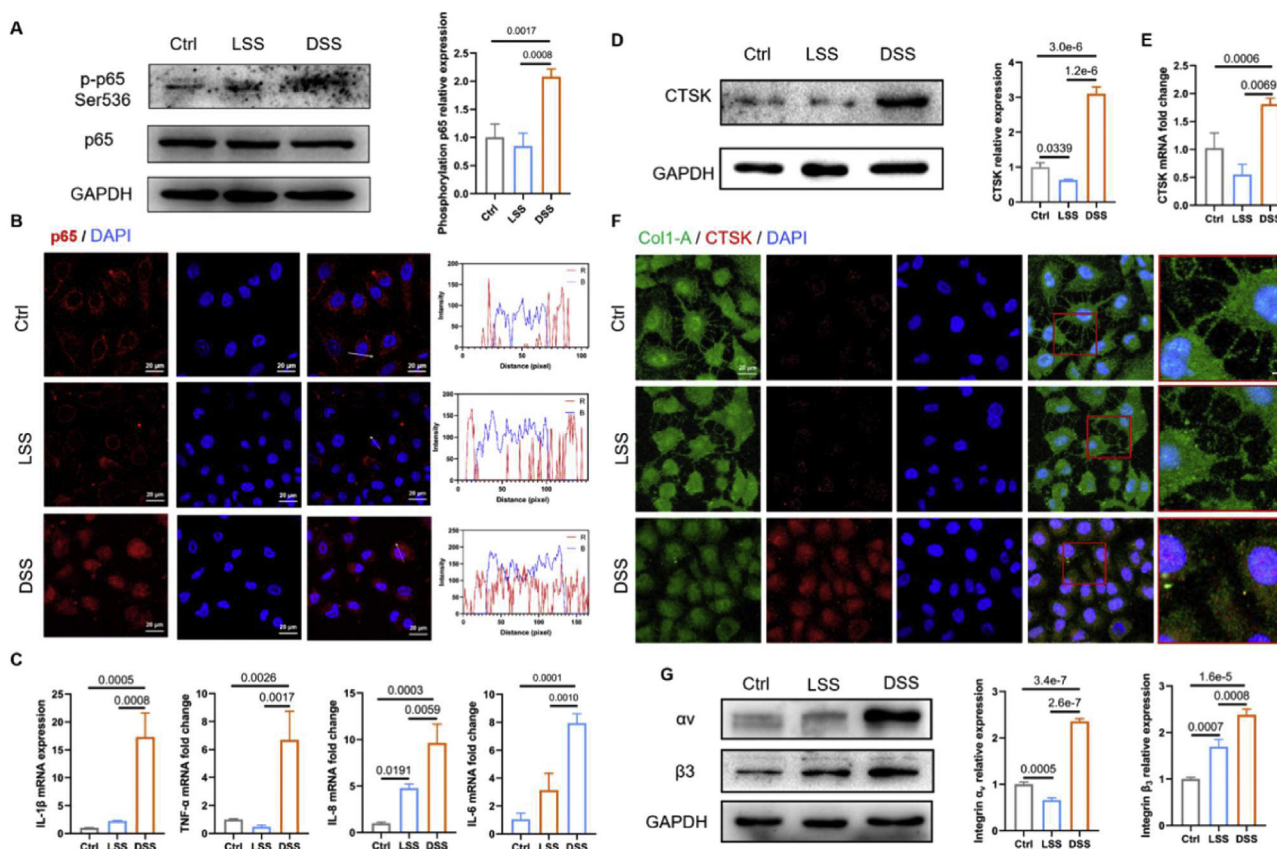


Figure 5 DSS induces endothelial inflammation and increases CTSK expression *in vitro*. (A) The Western blot of p65 and p-p65 in HUVECs were subject to different flows. The grayscale value was quantized by Image J software ($n = 3$). (B) Immunofluorescence images of p65 (red) in HUVECs under different flow conditions, the nucleus stained by DAPI, and the images captured by confocal microscopes (Scale bar: 20 μm). (C) The expression levels of mRNA (IL-1 β , IL-6, TNF- α , and IL-8) were measured by qRT-PCR in HUVECs exposed to different flow conditions ($n = 3$). (D, E) The related protein and mRNA expression levels of CTSK in HUVECs were exposed to different flow conditions for 8 hours ($n = 3$). (F) Immunofluorescence images of CTSK (red) and Col1-A (green) in HUVECs exposed to different flow conditions. Nuclei were stained with DAPI, and images were captured by confocal microscope (Scale bar: 20 μm). (G) The HUVECs were exposed to different flow conditions, and the total cell lysates were immunoblotted with integrin αv or β3 ($n = 3$).

Using I κ B/IKK inhibitors BAY 11–7085 (10 μM for 12 hours) we further investigate the effects of NF- κ B on the CTSK expression in HUVECs exposed to DSS or LSS. It could be found in Figure 6E, the expression of CTSK induced by DSS was significantly decreased by the inhibition of the activation of NF- κ B pathway.

Integrin blocking alleviate inflammation and remodeling in normolipidemic mice

Based on the above *in vitro* research results, the cell surface integrin receptor could serve as a potential therapeutic target. Therefore, we tested the anti-inflammation effects of integrin inhibitor cilengitide (5 $\mu\text{g}/\text{kg}/\text{d}$) in the carotid artery ligation model. As shown in Figure 7A, the expression of p-p65 was hindered by cilengitide in ligation normolipidemic mice. These results indicated that integrin blocking could decrease the vascular inflammation induced by the disturbed flow. H&E staining results demonstrated that cilengitide treatment could reduce the intima thickening in LCA regions (Fig. 7B). In addition, there was no

apparent rupture of elastin in LCA after administration of cilengitide (Fig. 7C). However, the number of elastin breaks in DA regions (LSS area) were increased after cilengitide administration compared with dimethyl sulfoxide vehicle control (1:1 solution of dimethyl sulfoxide: PBS) group (Fig. 7C).

Integrin blocking reduces disturbed flow-induced atherosclerosis

Based on the above promising results, we evaluated the athero-protective property of integrin blocking in fast atherosclerosis induced by the DSS. As shown in Figure 8A and B, the lipid deposition in the LCA and AA regions of hyperlipidemia mice with carotid artery ligation in the cilengitide treatment groups was significantly decreased than dimethyl sulfoxide vehicle control. Meanwhile, the expression of CTSK, measured by immunofluorescence images, in the atherosclerotic plaques was decreased after cilengitide administration (Fig. 8C). Additionally, we also found that the inhibition of integrin could decrease the co-

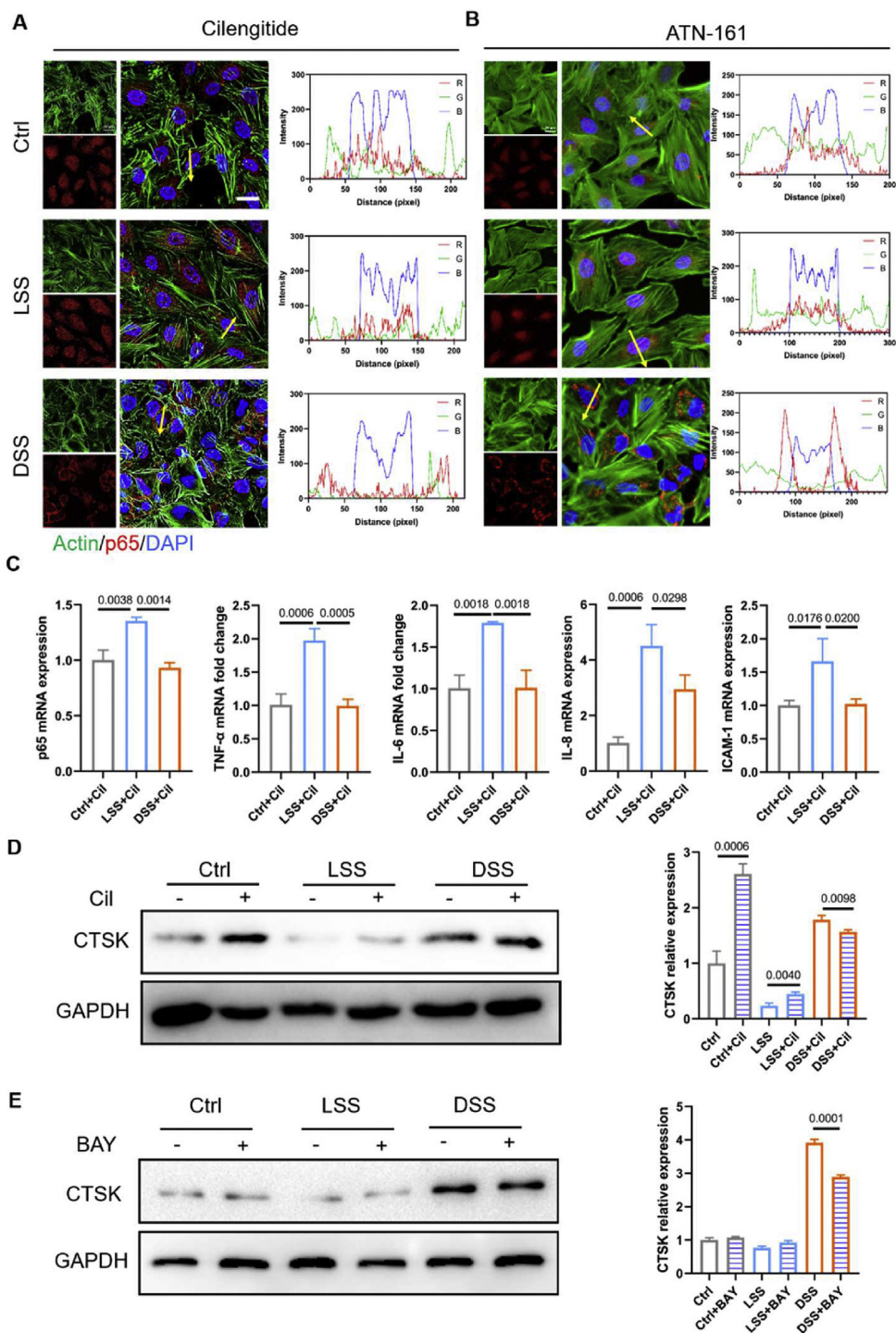


Figure 6 Disturbed flow induces endothelial cell inflammation depending on the integrin–NF- κ B axis. **(A)** Immunofluorescence images of p65 (red) and actin (green) on the HUVECs under different flow conditions in the presence of a specific inhibitor of integrin α v β 3 cilengitide (5 μ M for 12 hours), ATN-161 (5 μ M for 12 hours) **(B)**. Nuclei were stained with DAPI, and the images were captured by a confocal microscope (Scale bar: 20 μ m). **(C)** The pro-inflammatory mRNA expression in HUVECs, determined by qRT-PCR, under different flow conditions in the presence of integrin inhibitors cilengitide ($n = 3$). **(D)** HUVECs are subject to different flow conditions in the presence of integrin inhibitors cilengitide (5 μ M for 12 hours). Total cell lysates of treated cells were immunoblotted for CTSK, and GAPDH. The images were captured by Western blot imaging systems, and the quantitation were measured by Image J software ($n = 3$). **(E)** HUVECs are subject to different flow conditions in the presence of κ B/I κ B inhibitors BAY 11–7085 (10 μ M for 12 hours). Total cell lysates of treated cells were immunoblotted for CTSK, and GAPDH. The images were captured by Western blot imaging systems, and the quantitation was measured by Image J software ($n = 3$).

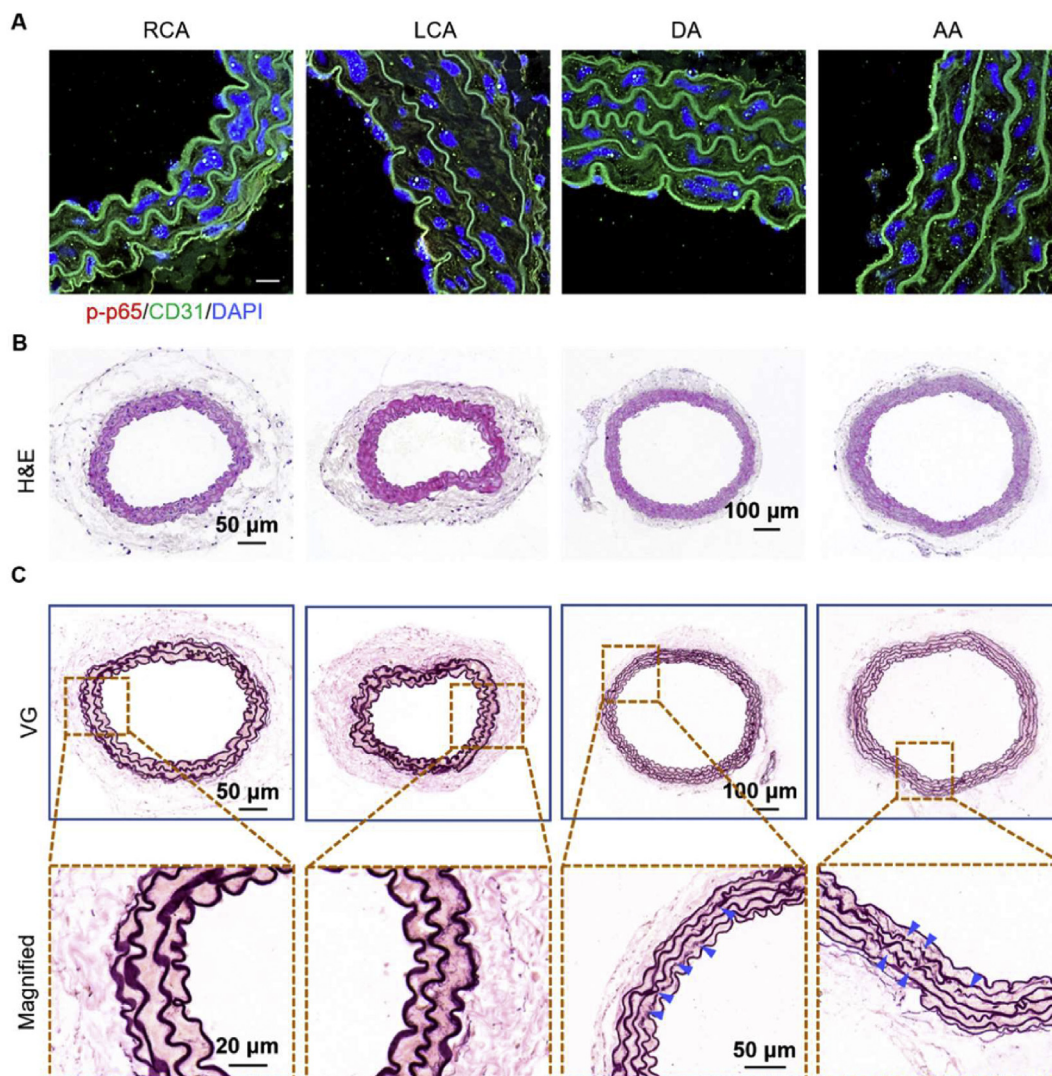


Figure 7 Integrin blocking alleviates inflammation and remodeling in normolipidemic mice. (A) Immunofluorescent staining for p-p65 (red) and CD31 (green) on the RCA, LCA, DA, and AA from normolipidemic mice 21 days after ligation administered with a specific inhibitor of integrin $\alpha v \beta 3$ cilengitide (5 $\mu\text{g}/\text{kg}/\text{d}$), respectively. Nuclei were stained with DAPI, and images were captured by confocal microscope (Scale bar: 20 μm). (B) H&E staining of RCA, LCA, DA, and AA sections from 21 days after ligation was administered with cilengitide (5 $\mu\text{g}/\text{kg}/\text{d}$). (C) VG staining of RCA, LCA, DA, and AA sections after blocked integrin by cilengitide *in vivo*, respectively (elastin rupture sites were shown in blue arrow).

localization of CTSK and Col1-A (Fig. S4). H&E staining results showed that integrin blocking could significantly reduce the progression of atherosclerotic plaques and vascular mean diameter in hyperlipidemia 21 days after ligation (Fig. 8D, E). In addition, the medial diameter and number of ruptures of elastin in LCA were decreased in the cilengitide administered groups compared with dimethyl sulfoxide vehicle control (Fig. 8F–H).

Discussion

Atherosclerosis is a chronic inflammatory disease, occurring preferentially in bifurcation, branching, and bending of blood vessels exposed to disturbed flow.²⁵ Atheroprone flow induces the formation of atherogenic endothelial phenotype and early atherosclerotic plaque through complex

mechanical-reception and mechanical–transduction processes to regulate endothelial gene expression.²⁶ Interestingly, this phenomenon is not independent, usually accompanied by vascular remodeling. The proliferation and migration of SMCs from medial to intimal are contributed to the intimal thickening induced by the disturbed flow.²⁷ The extracellular matrix components will be degraded during this process to provide space for smooth muscle migration. Matrix metalloproteinases,²⁸ cathepsin,²⁹ and angiotensin³⁰ are essential factors that can reshape the extracellular matrix and cause vascular remodeling. CTSK is one of the most potent proteases in lysosomal cysteine proteases belonging to the peptidase protein C1 family, mainly expressed in osteoclasts and involved in bone remodeling and resorption. In addition, CTSK has been reported to play an essential role in other diseases, such as keratinocyte

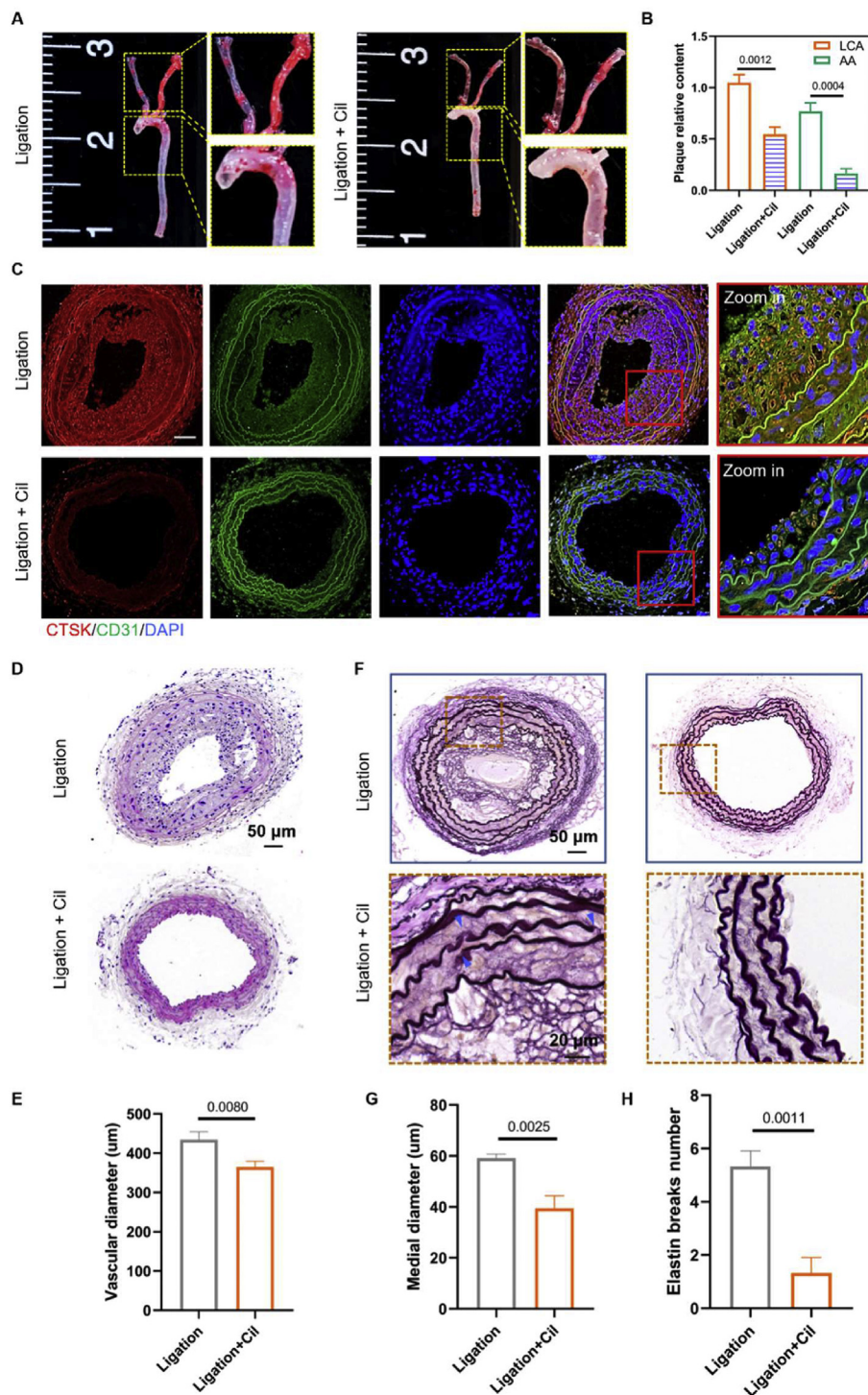


Figure 8 Integrin blocking reduces disturbed flow-induced atherosclerosis. (A) The arterial whole-mount ORO staining on the arteries was harvested 21 days after ligation from *ApoE*^{-/-} mice administrated with a specific inhibitor of integrin $\alpha v\beta 3$ cilengitide (5 $\mu\text{g}/\text{kg}/\text{d}$). (B) The lipid deposition in AA and LCA were quantified by Images J software ($n = 3$). (C) Immunofluorescence images of CTSK (red) and CD31 (green) in LCA from *ApoE*^{-/-} mice 21 days after ligation and administrated with cilengitide (5 $\mu\text{g}/\text{kg}/\text{d}$). DAPI stained the nucleus, and the images were captured by a confocal microscope (Scale bar: 20 μm). (D) H&E staining of LCA sections from *ApoE*^{-/-} mice 21 days after ligation and administrated with cilengitide (5 $\mu\text{g}/\text{kg}/\text{d}$). (E) The vascular mean diameter of LCA tissue sections was measured by Image J software ($n = 3$). (F) VG staining of LCA sections from *ApoE*^{-/-} mice 21 days after ligation, the sites of elastic breaks as indicated by blue arrows. (G) Medial diameter and (H) elastin break number of VG-stained LCA tissue sections were measured by Image J software ($n = 3$).

differentiation,³¹ tumor invasion and metastasis,³² congenital heart defects,³³ and atherosclerosis.¹¹ The primary function of CTSK is extracellular matrix degradation and remodeling and has potent collagenolytic activity against type I/II collagen. Furthermore, it is reported that CTSK regulates inflammation response through TLR-9²² and TGF- β ²³ signaling pathways. In this work, we reveal that the vascular inflammation caused by the disturbed flow could promote the expression of CTSK, which in turn leads to vascular remodeling.

Integrin is a transmembrane receptor that mediates the mechanic-chemical signal transport between the extracellular matrix (ECM) and the cytoskeleton.³⁴ Endothelial cells express different integrin receptors for mediating binding to the extracellular matrix. For example, the expression of integrin α 1 β 1 and α 2 β 1 binds to collagen, and the expression (α 3 β 1, α 6 β 1, and α 6 β 4) integrin binds to laminin in the natural state for anchoring to the extracellular matrix to maintain vascular homeostasis. In addition, endothelial cells also expressed integrins (including α 5 β 1 and α v β 3) that cause ECs activation for angiogenesis or pathological conditions. In the early stage of atherosclerosis, integrin α v β 3 is considered the main element that mediates the pro-inflammatory signals (NF- κ B) generated by the atheroprone flow.¹² The inhabitation of integrin α v β 3 or α v knockout could decrease the inflammation and plaques deposition in *ApoE*^{-/-} mice aorta. Notably, inhibition of other integrins (α 5^{35,36}, β 1¹⁹) subunits can also block the activation of endothelial cell inflammatory signals induced by the disturbed flow. However, we used laminar flow to stimulate HUVECs that have been inhibited by integrin and found the activation of NF- κ B and upgraded expression of inflammatory cytokines. In addition, we also observed more elastin breaks in laminar shear stress of vascular (such as DA) after treatment with integrin inhibitors. These results suggest that integrin may be a two-way switch that can sense laminar flow and disturbed flow, respectively, resulting in different inflammatory responses. Similar results have been observed by Vedanta et al³⁷; they found that a force sensor guidance receptor plexin D1 has binary functions to sense the upstream mechanical signals. The plaque areas in the aorta arch of plexin D1 knockout *ApoE*^{-/-} mice were significantly reduced compared to wild-type mice.³⁷ However, obvious plaque burden has been observed in the descending aorta areas in the plexin D1 knockout *ApoE*^{-/-} mice.

Interestingly, when we inhibit NF- κ B *in vitro*, the expression of CTSK decreases. Therefore, we believe that the CTSK may be regulated by NF- κ B signal. NF- κ B is a transcription factor belonging to the "Rel" family. It represents a critical intracellular signal transduction system and is involved in various inflammatory diseases, including atherosclerosis.³⁸ Inhibition of NF- κ B eliminates the induction of adhesion molecules in endothelial cells, disrupts the recruitment of macrophages to atherosclerotic plaques, and reduces the expression of cytokines and chemokines in the aorta.³⁹ Therefore, the strategies for local or endothelial-specific inhibition of NF- κ B may open up new therapeutic methods for preventing and treating this disease.

The actin cytoskeleton is a critical component of cells, which plays an essential role in regulating cell proliferation and migration. Studies have shown that the cytoskeleton is

closely related to the activation of NF- κ B.⁴⁰ For example, Crépieux et al⁴¹ found that the NF- κ B inhibitor, I κ B- α , physically binds to the microtubules, which is a component of the cytoskeleton. On the other hand, NF- κ B can be active by the Rho family, which is an important enzyme involved in regulating the structure of the actin cytoskeleton.⁴² In addition, Alexandra et al found that the p65 protein can bind to the filamentous actin.⁴³ In this study, we demonstrated that the inhibition of cytoskeleton polymerization with the treatment of LatB would further increase the retention of p65 protein in the cytoplasm in both static culture and LSS conditions; in the DSS condition, LatB will promote the p65 protein to enter the nucleus.

Conclusion

In conclusion, we demonstrated that the CTSK contributed to disturbed flow-induced endothelial inflammation and vascular remodeling, dependent on integrin α v β 3-cytoskeleton-NF- κ B signaling. Additionally, the inhibition of integrin α v β 3-cytoskeleton is promising as a target for vascular anti-inflammation and anti-atherosclerosis treatment.

Author contributions

FF performed most of the tests and analysis and wrote the manuscript. YS, and XHL came up with constructive proposals and revised the manuscript. WQ, TF involved in cellular molecular biology experiments. HYZ, and TF performed and analyzed experiments with animal samples. Data analysis and interpretation were done by JWJ, YDC and GXW. All authors discussed the results and implications and commented on the paper.

Conflict of interests

The authors declare that they have no known competing financial interests or personal relationships that could have appeared to influence the work reported in this paper.

Funding

This work was supported by The National Natural Science Foundation of China (No. 11932014, 32071312, 31870939, 31971239 and 12032007).

Appendix A. Supplementary data

Supplementary data to this article can be found online at <https://doi.org/10.1016/j.gendis.2022.03.020>

References

1. Gisterå A, Hansson GK. The immunology of atherosclerosis. *Nat Rev Nephrol.* 2017;13(6):368–380.
2. Albarrán-Juárez J, Iring A, Wang S, et al. Piezo1 and G q/G 11 promote endothelial inflammation depending on flow pattern and integrin activation. *J Exp Med.* 2018;215(10):2655–2672.

3. Souilhol C, Serbanovic-Canic J, Fragiadaki M, et al. Endothelial responses to shear stress in atherosclerosis: a novel role for developmental genes. *Nat Rev Cardiol.* 2020;17(1):52–63.
4. Renna NF, de Las Heras N, Miatello RM. Pathophysiology of vascular remodeling in hypertension. *Int J Hypertens.* 2013;2013:808353.
5. Bai L, Lutgens E, Heeneman S. Cathepsins in Atherosclerosis. In: George SJ, Johnson J, eds. *Atherosclerosis: Molecular and Cellular Mechanisms.* Weinheim: Wiley-VCH Verlag GmbH & Co. KGaA; 2010:173–191.
6. Hofnagel O, Robenek H. Cathepsin K: boon or bale for atherosclerotic plaque stability? *Cardiovasc Res.* 2009;81(2):242–243.
7. Barascuk N, Skjøtt-Arkil H, Register TC, et al. Human macrophage foam cells degrade atherosclerotic plaques through cathepsin K mediated processes. *BMC Cardiovasc Disord.* 2010;10(1):19.
8. Sun Y, Ishibashi M, Seimon T, et al. Free cholesterol accumulation in macrophage membranes activates Toll-like receptors and p38 mitogen-activated protein kinase and induces cathepsin K. *Circ Res.* 2009;104(4):455–465.
9. Jiang H, Cheng XW, Shi GP, et al. Cathepsin K-mediated Notch1 activation contributes to neovascularization in response to hypoxia. *Nat Commun.* 2014;5:3838.
10. Lügering N, Kucharzik T, Stein H, et al. IL-10 synergizes with IL-4 and IL-13 in inhibiting lysosomal enzyme secretion by human monocytes and lamina propria mononuclear cells from patients with inflammatory bowel disease. *Dig Dis Sci.* 1998;43(4):706–714.
11. Liu CL, Guo J, Zhang X, et al. Cysteine protease cathepsins in cardiovascular disease: from basic research to clinical trials. *Nat Rev Cardiol.* 2018;15(6):351–370.
12. Chen J, Green J, Yurdagul Jr A, et al. $\alpha v \beta 3$ integrins mediate flow-induced NF- κB activation, pro-inflammatory gene expression, and early atherogenic inflammation. *Am J Pathol.* 2015;185(9):2575–2589.
13. Li F, Yan K, Wu L, et al. Single-cell RNA-seq reveals cellular heterogeneity of mouse carotid artery under disturbed flow. *Cell Death Dis.* 2021;7(1):180.
14. Zhang K, Chen Y, Zhang T, et al. A novel role of Id1 in regulating oscillatory shear stress-mediated lipid uptake in endothelial cells. *Ann Biomed Eng.* 2018;46(6):849–863.
15. Sun J, Luo Q, Liu L, et al. Low-level shear stress promotes migration of liver cancer stem cells via the FAK-ERK1/2 signalling pathway. *Cancer Lett.* 2018;427:1–8.
16. Yu H, He J, Su G, et al. Fluid shear stress activates YAP to promote epithelial-mesenchymal transition in hepatocellular carcinoma. *Mol Oncol.* 2021;15(11):3164–3183.
17. Zampetaki A, Zeng L, Margariti A, et al. Histone deacetylase 3 is critical in endothelial survival and atherosclerosis development in response to disturbed flow. *Circulation.* 2010;121(1):132–142.
18. Martin D, Li Y, Yang J, et al. Unspliced X-box-binding protein 1 (XBP1) protects endothelial cells from oxidative stress through interaction with histone deacetylase 3. *J Biol Chem.* 2014;289(44):30625–30634.
19. Hu S, Liu Y, You T, et al. Vascular semaphorin 7A upregulation by disturbed flow promotes atherosclerosis through endothelial $\beta 1$ integrin. *Arterioscler Thromb Vasc Biol.* 2018;38(2):335–343.
20. Qin X, Zhang K, Qiu J, et al. Uptake of oxidative stress-mediated extracellular vesicles by vascular endothelial cells under low magnitude shear stress. *Bioact Mater.* 2021;9:397–410.
21. Shi N, Mei X, Chen SY. Smooth muscle cells in vascular remodeling. *Arterioscler Thromb Vasc Biol.* 2019;39(12):e247–e252.
22. Wei W, Ren J, Yin W, et al. Inhibition of Ctsk modulates periodontitis with arthritis via downregulation of TLR9 and autophagy. *Cell Prolif.* 2020;53(1):e12722.
23. Zhang X, Zhou Y, Yu X, et al. Differential roles of cysteinyl cathepsins in TGF- β signaling and tissue fibrosis. *iScience.* 2019;19:607–622.
24. Yamashiro Y, Yanagisawa H. The molecular mechanism of mechanotransduction in vascular homeostasis and disease. *Clin Sci.* 2020;134(17):2399–2418.
25. Demos C, Williams D, Jo H. Disturbed flow induces atherosclerosis by annexin A2-mediated integrin activation. *Circ Res.* 2020;127(8):1091–1093.
26. Chatzizisis YS, Coskun AU, Jonas M, et al. Role of endothelial shear stress in the natural history of coronary atherosclerosis and vascular remodeling: molecular, cellular, and vascular behavior. *J Am Coll Cardiol.* 2007;49(25):2379–2393.
27. Sho M, Sho E, Singh TM, et al. Subnormal shear stress-induced intimal thickening requires medial smooth muscle cell proliferation and migration. *Exp Mol Pathol.* 2002;72(2):150–160.
28. Galis ZS, Khatri JJ. Matrix metalloproteinases in vascular remodeling and atherogenesis: the good, the bad, and the ugly. *Circ Res.* 2002;90(3):251–262.
29. Donners MMPC, Bai L, Lutgens SPM, et al. Cathepsin K deficiency prevents the aggravated vascular remodeling response to flow cessation in ApoE-/- mice. *PLoS One.* 2016;11(9):e0162595.
30. Lu Y, Sun X, Peng L, et al. Angiotensin II-Induced vascular remodeling and hypertension involves cathepsin L/V- MEK/ERK mediated mechanism. *Int J Cardiol.* 2020;298:98–106.
31. Rüniger TM, Quintanilla-Dieck MJ, Bhawan J. Role of cathepsin K in the turnover of the dermal extracellular matrix during scar formation. *J Invest Dermatol.* 2007;127(2):293–297.
32. Li R, Zhou R, Wang H, et al. Gut microbiota-stimulated cathepsin K secretion mediates TLR4-dependent M2 macrophage polarization and promotes tumor metastasis in colorectal cancer. *Cell Death Differ.* 2019;26(11):2447–2463.
33. Lu PN, Moreland T, Christian CJ, et al. Inappropriate cathepsin K secretion promotes its enzymatic activation driving heart and valve malformation. *JCI Insight.* 2020;5(20):e133019.
34. Sun Z, Guo SS, Fässler R. Integrin-mediated mechanotransduction. *J Cell Biol.* 2016;215(4):445–456.
35. Yurdagul Jr A, Green J, Albert P, et al. $\alpha 5 \beta 1$ integrin signaling mediates oxidized low-density lipoprotein-induced inflammation and early atherosclerosis. *Arterioscler Thromb Vasc Biol.* 2014;34(7):1362–1373.
36. Budatha M, Zhang J, Zhuang ZW, et al. Inhibiting integrin $\alpha 5$ cytoplasmic domain signaling reduces atherosclerosis and promotes arteriogenesis. *J Am Heart Assoc.* 2018;7(3):e007501.
37. Mehta V, Pang KL, Rozbesky D, et al. The guidance receptor plexin D1 is a mechanosensor in endothelial cells. *Nature.* 2020;578(7794):290–295.
38. Pamukcu B, Lip GYH, Shantsila E. The nuclear factor- κB pathway in atherosclerosis: a potential therapeutic target for atherothrombotic vascular disease. *Thromb Res.* 2011;128(2):117–123.
39. Gareus R, Kotsaki E, Xanthoulea S, et al. Endothelial cell-specific NF- κB inhibition protects mice from atherosclerosis. *Cell Metabol.* 2008;8(5):372–383.
40. Fazal F, Minhajuddin M, Bijli KM, et al. Evidence for actin cytoskeleton-dependent and-independent pathways for RelA/p65 nuclear translocation in endothelial cells. *J Biol Chem.* 2007;282(6):3940–3950.
41. Crépieux P, Kwon H, Leclerc N, et al. I κB α physically interacts with a cytoskeleton-associated protein through its signal response domain. *Mol Cell Biol.* 1997;17(12):7375–7385.
42. Perona R, Montaner S, Saniger L, et al. Activation of the nuclear factor- κB by Rho, CDC42, and Rac-1 proteins. *Genes Dev.* 1997;11(4):463–475.
43. Are AF, Galkin VE, Pospelova TV, et al. The p65/RelA subunit of NF- κB interacts with actin-containing structures. *Exp Cell Res.* 2000;256(2):533–544.